Water Research 252 (2024) 121146

Contents lists available at ScienceDirect

Water Research

journal homepage: www.elsevier.com/locate/watres

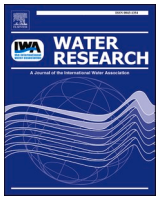

# Biotransformation of 6:2 fluorotelomer sulfonate and microbial community dynamics in water-saturated one-dimensional flow-through columns

Peng-Fei Yan [a,1,*], Sheng Dong [a,1], Matthew J. Woodcock [b], Katherine E. Manz [c], Uriel Garza-Rubalcava [b], Linda M. Abriola [b], Kurt D. Pennell [b], Natalie L. Cápiro [a,*]

[a] Department of Biological and Environmental Engineering, Cornell University, Ithaca, NY, United States
[b] School of Engineering, Brown University, Providence, RI, United States
[c] School of Public Health, University of Michigan, Ann Arbor, MI, United States

ARTICLE INFO

*Keywords:*
6:2 FTS
Fluorotelomer sulfonate
AFFF
PFAS
Biotransformation
Microbial community
Groundwater contaminant transport
Mathematical modeling

ABSTRACT

Nearly all per- and polyfluoroalkyl substances (PFAS) biotransformation studies reported to date have been limited to laboratory-scale batch reactors. The fate and transport of PFAS in systems that more closely represent field conditions, i.e., in saturated porous media under flowing conditions, remain largely unexplored. This study investigated the biotransformation of 6:2 fluorotelomer sulfonate (6:2 FTS), a representative PFAS of widespread environmental occurrence, in one-dimensional water-saturated flow-through columns packed with soil obtained from a PFAS-contaminated site. The 305-day column experiments demonstrated that 6:2 FTS biotransformation was rate-limited, where a decrease in pore-water velocity from 3.7 to 2.4 cm/day, resulted in a 21.7–26.1 % decrease in effluent concentrations of 6:2 FTS and higher yields (1.0–1.4 mol% vs. 0.3 mol%) of late-stage biotransformation products ($C_4$–$C_7$ perfluoroalkyl carboxylates). Flow interruptions (2 and 7 days) were found to enhance 6:2 FTS biotransformation during the 6–7 pore volumes following flow resumption. Model-fitted 6:2 FTS column biotransformation rates (0.039–0.041 $cm^3_w/g_s/d$) were ~3.5 times smaller than those observed in microcosms (0.137 $cm^3_w/g_s/d$). Additionally, during column experiments, planktonic microbial communities remained relatively stable, whereas the composition of the attached microbial communities shifted along the flow path, which may have been attributed to oxygen availability and the toxicity of 6:2 FTS and associated biotransformation products. Genus *Pseudomonas* dominated in planktonic microbial communities, while in the attached microbial communities, *Rhodococcus* decreased and *Pelotomaculum* increased along the flow path, suggesting their potential involvement in early- and late-stage 6:2 FTS biotransformation, respectively. Overall, this study highlights the importance of incorporating realistic environmental conditions into experimental systems to obtain a more representative assessment of *in-situ* PFAS biotransformation.

## 1. Introduction

Per- and polyfluoroalkyl substances (PFAS) have been extensively used for more than 50 years in a variety of commercial and industrial products (Buck et al., 2011), including aqueous film-forming foams (AFFFs) manufactured to effectively extinguish hydrocarbon-based fuel fires (Moody and Field, 2000). As a result, PFAS contamination is found in surface waters, groundwater, soils, and biota throughout the world (Ahrens et al., 2015; Prevedouros et al., 2006), and concern over the negative impacts of PFAS contamination on environmental and human health is growing (Grandjean and Clapp, 2015). Upon release into the soil environment, the fate of PFAS can be affected by numerous processes, such as recharge rate, sorption, and abiotic/biotic transformation. Understanding the role of these processes in the environmental fate and transport of PFAS will allow for effective management and remediation of contaminated sites.

Microbial transformation of PFAS, primarily in the form of polyfluoroalkyl substances (referred to hereafter as precursors), has been the subject of increasing study in recent years. Laboratory investigations demonstrated that microorganisms present in river sediments (Zhang et al., 2016) and surface soils (Liu et al., 2021) were capable of biotransforming several classes of precursors. The biotransformation of

* Corresponding authors at: Department of Biological and Environmental Engineering, Cornell University, 111 Wing Dr., Ithaca, NY 14853, United States.
*E-mail addresses:* py222@cornell.edu (P.-F. Yan), natalie.capiro@cornell.edu (N.L. Cápiro).
[1] These authors contributed equally to this work.

https://doi.org/10.1016/j.watres.2024.121146
Received 31 October 2023; Received in revised form 10 January 2024; Accepted 14 January 2024
Available online 15 January 2024

precursors often results in the formation of perfluoroalkyl acids (PFAAs), which are of particular concern due to their persistence, toxicity, and bioaccumulation potential (Houtz et al., 2013; Nelson et al., 2010). Some compounds such as fluorotelomer acids that are more toxic than their PFAA counterparts (Mitchell et al., 2011), can also be formed following biotransformation processes (Hamid et al., 2020; Zhang et al., 2016). These findings indicate that accounting for biotransformation processes is crucial for assessment of the environmental fate of precursors, as well as their potential effects on environmental and human health.

Despite an improved understanding of precursor biotransformation processes, nearly all previous studies were conducted in laboratory-scale batch reactors (Dong et al., 2023; Hamid et al., 2020; Liu et al., 2021; Yan et al., 2022). Batch reactors can be static or well-mixed systems, both of which lack the representation of crucial field conditions such as the presence of groundwater flow. In addition, the solid-to-water ratio is typically much smaller in batch reactors (e.g., < 50% g solid/g water) than those encountered in subsurface environments, where the solid-to-water ratio typically exceeds 80% wt. Previous studies have revealed discrepancies between the biodegradation rates of organic contaminants (e.g., chlorinated ethenes) in batch reactor and column experiments (Grösbacher et al., 2018; Schaefer et al., 2009). However, there is an absence of studies investigating PFAS precursor biotransformation in dynamic column or larger-scale systems. Such studies will be critical to advance our understanding of the impacts of biotransformation on the fate and transport of precursors in natural environments.

To fill these knowledge gaps, this study investigated the biotransformation of 6:2 fluorotelomer sulfonate (6:2 FTS), which was selected as a representative precursor given its widespread detection at AFFF-impacted sites (Ahrens et al., 2015; Houtz et al., 2013), in one-dimensional (1-D) flow-through columns packed with soil obtained from a PFAS-contaminated site. Prior batch reactor studies demonstrated that 6:2 FTS could be transformed by microorganisms in river sediment and landfill leachate (Hamid et al., 2020; Zhang et al., 2016). However, the fate and transport of 6:2 FTS has not yet been investigated in dynamic experimental systems that incorporate groundwater flow. Further, it is unknown whether 6:2 FTS biotransformation is rate-limited and would be impacted by hydraulic residence time. In this study, dynamic flow conditions, including two different pore-water velocities and periods of flow interruption, were applied to evaluate the associated mass-transfer impacts on the biotransformation of 6:2 FTS. Biotransformation rates, extent, and pathways of 6:2 FTS in the columns were also compared to prior microcosm studies (Yan et al., 2024) to gain insights into the potential impact of system scale, solid-to-water ratio and/or flow conditions on precursor biotransformation. Moreover, the dynamics and distribution of native microbial communities in the aqueous and solid phases throughout the columns were investigated. Microbial taxa that were potentially responsible for 6:2 FTS biotransformation were identified.

## 2. Materials and methods

### 2.1. Column design and preparation

Customized borosilicate glass chromatography columns (2.5 cm inner diameter, 15 cm length; Kimble-Chase, Vineland, NJ) equipped with three glass sampling ports sealed with rubber septa (Restek, Bellefonte, PA) were used in this study. Ports 1 and 3 were located 3.5 cm from the column influent and effluent endplates, respectively, and port 2 was located at the column midpoint (Fig. 1). All column components

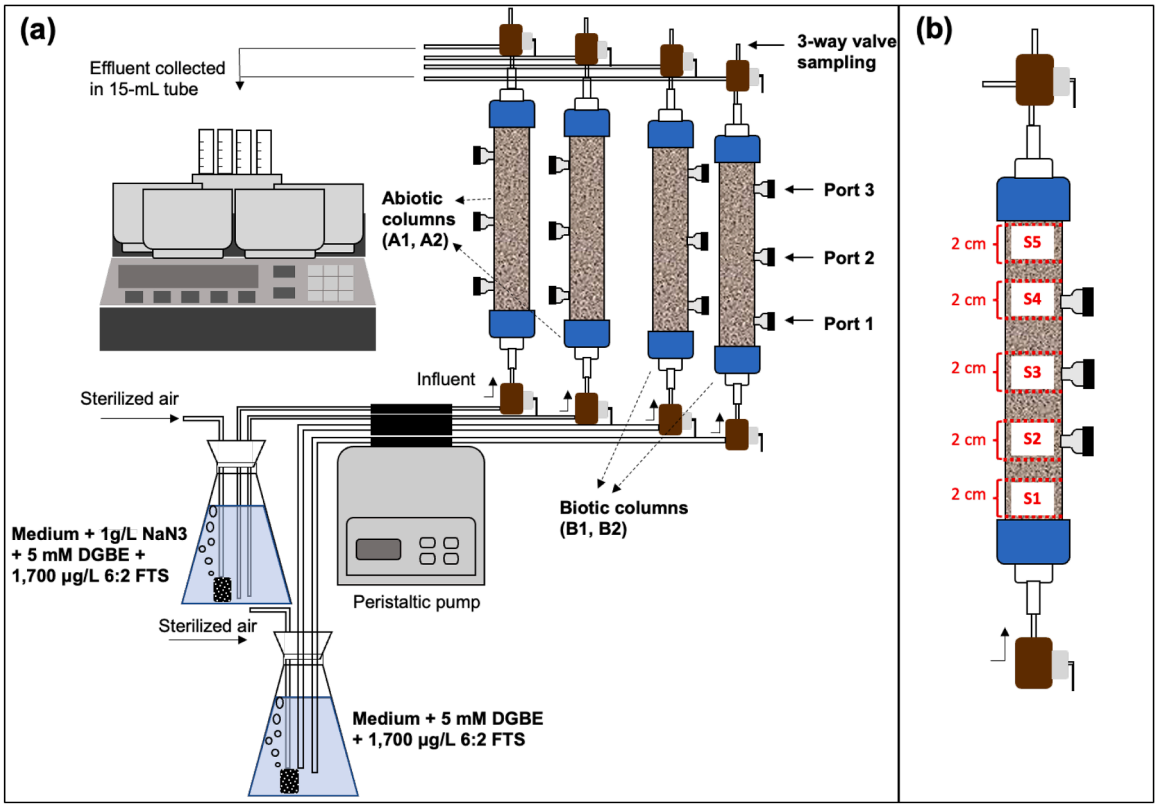


**Fig. 1.** Schematic diagrams of (a) column experimental set-up. Four borosilicate glass columns (2.5 cm inner diameter, 15 cm length) were identically packed with mixed Loring soil and Federal Fine sand (1:1, w/w). Biotic and abiotic (with additional 1 g/L sodium azide) column influent were aerated and introduced to duplicate biotic and abiotic columns, respectively, via a peristaltic pump. (b) Segments S1-S5 delineated for the dissection of solid phase at the termination of column experiments. Segment S1 was closest to the column inlet, and segment S5 was closest to the column outlet. Ports 1, 2, and 3 were located at the center of segments S2, S3, and S4, respectively.

were either autoclaved (121 °C, 30 min) or washed with 70 % isopropyl alcohol for sterilization prior to use. A total of four columns were packed with mixed Federal Fine sand and an AFFF-impacted soil collected from the former Loring Air Force Base (Aroostook County, ME) (1:1, w/w). Detailed information on the porous media used in this study is provided in the Supplementary Material (SM)-Section S1. Columns were packed by alternating the addition of 1-cm porous media with vibration and manual compression. Following packing, columns were purged with $CO_2$ gas to facilitate dissolution of entrapped air, then saturated with sterile synthetic groundwater (see SM-Section S1 for details) in an up-flow mode. A non-reactive tracer test (20 mM sodium bromide, flow rate = 0.04 mL/min) was completed for each column following water saturation.

### 2.2. Column operation and sampling

Column experiments were initiated by introducing influent solutions (SM-Section S1) to duplicate abiotic and biotic columns (Fig. 1a). Four columns were packed identically with a pore volume (PV) of 28.9 ± 0.3 mL and a porosity of 0.35 ± 0.00 $cm^3/cm^3$. The influent was constantly aerated by bubbling sterilized air using an aquarium air pump (Imagitarium, San Diego, CA), and delivered to the columns via a peristaltic pump (Gilson Miniplus 3; Middleton, WI) in an up-flow mode (Fig. 1a). Column experiments were performed in two phases; in Phase I (0–33.1 PVs), the influent was introduced to the columns at a flow rate of 5.0 ± 0.1 μL/min, equivalent to a pore-water velocity ($v_p$) of 3.7 ± 0.2 cm/day and a hydraulic residence time (RT) of 4.1 ± 0.2 days. A 2-day flow interruption was conducted at 11.5 PVs. In Phase II (33.1–58.8 PVs), the flow rate was reduced to 3.2 ± 0.1 μL/min ($v_p$ = 2.4 ± 0.1 cm/day, RT = 6.3 ± 0.3 days), and a 7-day flow interruption was conducted at 47.4 PVs. Overall, all columns were operated for a total of 305 days (136 days in Phase I, and 169 days in Phase II).

Throughout the 305-day operation, column effluent was continuously collected in 15-mL centrifuge tubes (Fig. 1a). The effluent samples were used for the measurement of flow rate, fluoride ion (SM-Section S1), and dissolved organic carbon (DOC) (SM-Section S2). In addition, 65 μL of column effluent were collected from the 3-way valve (Fig. 1a) every PV (see Table S1 for the overview of experimental sampling events), and immediately mixed with methanol (1,235 μL) to minimize potential loss of volatile PFAS. The methanol-diluted sample was then filtered through a 0.45-μm Whatman GD/X glass microfiber filter (GMF) syringe filter (GE Healthcare, Chicago, IL), and stored at −20 °C prior to PFAS analysis. To investigate the biotransformation of 6:2 FTS along the flow path, additional aqueous samples were withdrawn from side-ports on the biotic columns (Ports 1–3, see Fig. 1a) at selected time points (Table S1) using a Chemyx Fusion 200 syringe pump (Chemyx Inc.; Stafford, TX) and 1-mL syringe (BD Luer-Lok) at a 10 % of background flow rate. The withdrawn sample (65 μL) was mixed with methanol (1,235 μL), filtered, and stored at −20 °C until PFAS analysis.

To confirm oxic conditions throughout the biotic columns, 1.5-mL samples were withdrawn from side-ports at selected time points (Table S1) for measurement of oxidation–reduction potential (ORP) (SM-Section S2). Additionally, 1-mL samples were collected from side-ports during Phase I and Phase II (Table S1) for biomass DNA extraction. At the termination of column experiments, biotic columns were destructively sampled to allow for the investigation of microbial community distribution in the solid phase. Each column was divided into five segments, S1-S5 (Fig. 1b), and the solid phase in each segment was transferred to a sterile 50-mL centrifuge tube using a flame-sterilized stainless-steel spatula. For the microbial community analysis, approximately 0.25 g of solids in each segment was used for DNA extraction (See Section 2.4).

### 2.3. PFAS analysis

Target PFAS analytes for LC-MS/MS analysis are listed in Table S2. Detection was achieved using a Waters ACQUITY ultra high-performance liquid chromatograph coupled with a Waters Xevo triple quadrupole mass spectrometer (UPLC-MS/MS) (Waters Corporation, Milford, MA). The UPLC was equipped with a Waters ACQUITY UPLC BEH C18 Column (130 Å, 1.7 μm, 2.1 mm X 50 mm). Details on the solvent gradient, instrumental parameters, and detection limits of target PFAS were previously documented in an earlier study (Yan et al., 2024).

### 2.4. DNA extraction and Illumina MiSeq sequencing

DNA extractions of aqueous side-port samples and solid samples from column segments S1-S5 were conducted using DNeasy PowerSoil Pro-Kit (Qiagen, Hilden, Germany) according to manufacturer protocols. Amplification and sequencing of DNA samples were performed at the Alkek Center for Metagenomics and Microbiome Research at Baylor College of Medicine. Detailed procedures are described in the prior study (Yan et al., 2024).

### 2.5. Mathematical modeling

The disappearance of 6:2 FTS was modeled as first-order in terms of both 6:2 FTS and biomass concentrations, mirroring Monod kinetics at low substrate concentration (Han and Levenspiel, 1988). Given that the growth of various microorganisms was not tracked, it was assumed that the biomass capable of transforming 6:2 FTS remained constant and proportional to the amount of soil. Thus, the reaction rate was expressed as:

$$r = -kC_sC \tag{1}$$

where $r$ is the rate of 6:2 FTS consumption per total volume ($M/L^3/T$), $k$ is the reaction rate coefficient ($L_w^3/M_S/T$), $C_s$ ($M_S/L^3$) is the mass of soil per total volume (constant in all columns), and $C$ ($M/L_w^3$) is the aqueous concentration of 6:2 FTS.

For modeling of transport and transformation of 6:2 FTS in the columns, the reaction rate expression (Equation 1) was incorporated into a 1-D advective-dispersive reactive transport equation:

$$(\theta + \rho_b K_d)\frac{\partial C}{\partial t} + \frac{\partial}{\partial z}\left(\theta v_p C - \theta D\frac{\partial C}{\partial z}\right) = -kC_sC \tag{2}$$

where $z$ (L) is the distance along the flow path, $\rho_b$ ($M/L^3$) is the bulk density of solids, $K_d$ ($L_w^3/M$) is the linear partition coefficient of 6:2 FTS, $\theta$ ($L_w^3/L^3$) is the porosity, $D$ is the diffusion/dispersion coefficient ($L^2/T$), and $v_p$ (L/T) is the average pore-water velocity. Note that, for evaluation of the microbial transformation term in Equations (1) and (2), the mass of soil per total volume is given by $C_s = \rho_b\varphi_s$, where $\varphi_s$is the mass fraction of soil in the solid phase.

The solution of Equation (2) requires initial and boundary conditions. If the column is free of 6:2 FTS at $t = 0$, the initial condition is $C(0, z) = 0$. The conditions representing flux continuity at the boundaries are given by:

$$v_pC_{in} = v_pC(t,0) - D\frac{\partial C(t,0)}{\partial z} \tag{3a}$$

$$\frac{\partial C(t,H)}{\partial z} = 0 \tag{3b}$$

where $C_{in}$ is the influent 6:2 FTS concentration and $H$ is the length of the column. The solution to Equation (2) with the initial and boundary conditions presented above was obtained numerically using the function pdepe in Matlab® with a grid size of $\Delta z = 0.15$ cm, and restricting the maximum time step to $\Delta t = 0.1$ $d$. For the steady-state conditions, the analytical solution of Equation (2) (SM-Section S3) was used to estimate the reaction rate coefficient using the non-linear solver fsolve in Matlab®.

## 3. Results and discussion

### 3.1. Biotransformation of 6:2 FTS under dynamic flow conditions

Throughout the 305-day experiments, 6:2 FTS in the effluent of both abiotic columns remained relatively constant (98.8 ± 10.5 mol% of spiked 6:2 FTS in the influent) after breakthrough (i.e., increased from 1.2 ± 0.0 mol% at 0.5 PVs to 103.8 ± 9.3 mol% at 2.5 PVs), indicating that 6:2 FTS was stable under the abiotic column conditions (Fig. 2). In contrast, a substantial decrease in 6:2 FTS concentrations was measured in the effluent of both biotic columns (Fig. 2). PFAS analysis also revealed the production of eight compounds only in the biotic columns (Fig. 3), confirming the occurrence of 6:2 FTS biotransformation under the biotic column conditions. The biotransformation products included 6:2 fluorotelomer saturated carboxylic acid (6:2 FTCA), 6:2 fluorotelomer unsaturated carboxylic acid (6:2 FTUA), 5:2 secondary fluorotelomer alcohol (5:2 sFTOH), 5:3 fluorotelomer carboxylic acid (5:3 acid), perfluorobutanoic acid (PFBA), perfluoropentanoic acid (PFPeA), perfluorohexanoic acid (PFHxA), and perfluoroheptanoic acid (PFHpA). To facilitate understanding of the biotransformation of 6:2 FTS in the column experiments, the eight products were divided into three classes: early-stage products (6:2 FTCA and 6:2 FTUA), middle-stage products (5:2 sFTOH and 5:3 acid), and late-stage products (PFBA, PFPeA, PFHxA, and PFHpA), based on proposed biotransformation pathways (Yan et al., 2024) (Fig. S1).

#### 3.1.1. Profiles of 6:2 FTS and biotransformation products in biotic column effluents

Based on the biotransformation of 6:2 FTS observed in the biotic columns, the column operations in Phase I ($v_p$ = 3.7 ± 0.2 cm/day) and Phase II ($v_p$ = 2.4 ± 0.1 cm/day) were further divided into three subphases (Phases I-A, I-B, and I-C, and Phases II-A, II-B, and II-C; Figs. 2 and 3). In Phase I-A (0.5–11.5 PVs), the breakthrough of 6:2 FTS was first observed (0.5–2.5 PVs), followed by a slow decrease in 6:2 FTS (Fig. 2), as well as an increasing formation of biotransformation products, especially early-stage products during 2.5–11.5 PVs (Fig. 3). Specifically, 6:2 FTS decreased from 95.0 ± 0.7 mol% at 2.5 PVs to 84.6 ± 4.2 mol% at 7.5 PVs, then further decreased to 78.5 ± 13.0 mol% at 11.5 PVs (Fig. 2). Correspondingly, the combined molar yields of 6:2 FTCA and 6:2 FTUA increased from 1.9 ± 1.5 mol% at 2.5 PVs to 6.6 ± 5.0 mol% at 7.5 PVs, then further increased to 18.1 ± 4.3 mol% at 11.5 PVs (Fig. 3). The formation of late-stage products during Phase I-A was minimal, except for PFHxA, which was produced with 0.3 ± 0.1 mol% at 11.5 PVs (Fig. 3). Taken together, these results indicate that 6:2 FTS biotransformation was initiated in Phase I-A, and the extent of biotransformation gradually increased, which might be attributed to the acclimation of native soil microorganisms under column conditions.

At 11.5 PVs, a 2-day flow interruption was conducted for all columns. After resuming flow, a sharp decrease in 6:2 FTS was measured (32.0 ± 7.1 mol% of 6:2 FTS at 14.5 PVs), followed by a partial rebound (61.4 ± 13.8 mol% at 17.5 PVs) in both biotic columns (Fig. 2). A similar decrease was not detected in abiotic columns (Fig. 2), indicating that 6:2 FTS sorption was not rate-limited under the studied column conditions. During Phase I-B (11.5–17.5 PVs), a greater formation of late-stage products and less production of early-stage products were observed than that observed in Phase I-A (Fig. 3), suggesting that a greater extent of 6:2 FTS biotransformation likely occurred in Phase I-B following the 2-day flow interruption. For example, PFBA and PFHpA were not produced in Phase I-A; however, both were formed with an average molar yield of 0.1 ± 0.1 mol% during Phase I-B (Fig. 3).

During 17.5–33.1 PVs (Phase I-C), a relatively constant concentration of 6:2 FTS was measured in the effluent of the biotic columns (Fig. 2). Similarly, the formation of 6:2 FTS biotransformation products appeared to be stable (Fig. 3). Therefore, the biotransformation of 6:2 FTS likely reached a steady-state in Phase I-C under the tested conditions (i.e., $v_p$ = 3.7 ± 0.2 cm/day). Under this steady-state, 70.8 ± 11.9 mol% of 6:2 FTS remained in the effluent of the biotic columns, along with average molar yields of 5.2 ± 3.8 mol% for 6:2 FTCA, 5.1 ± 2.5 mol% for 6:2 FTUA, 3.8 ± 3.2 mol% for 5:2 sFTOH, 2.0 ± 1.9 mol% for 5:3 acid, 0.0 ± 0.1 mol% for PFBA, 0.1 ± 0.1 mol% for PFPeA, 0.2 ± 0.2 mol

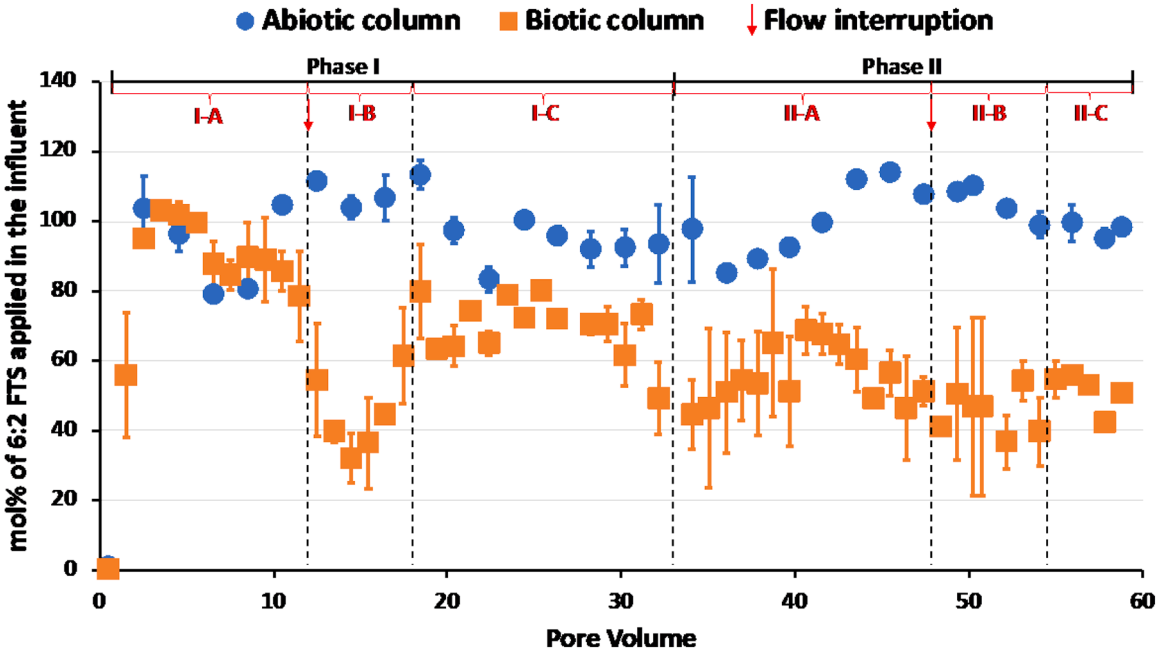


**Fig. 2.** Time-course of effluent 6:2 FTS molar percent during the operation of abiotic and biotic columns (Phase I and Phase II). Influent was introduced to the columns at a flow rate of 5.0 ± 0.1 μL/min, equivalent to a pore-water velocity ($v_p$) of 3.7 ± 0.2 cm/day and a hydraulic residence time (RT) of 4.1 ± 0.2 days in Phase I (0–33.1 PVs). Flow rate was reduced to 3.2 ± 0.1 μL/min ($v_p$ = 2.4 ± 0.1 cm/day, RT = 6.3 ± 0.3 days) during Phase II (33.1–58.8 PVs). Downward arrows represent the 2-day and 7-day flow-interruptions conducted at 11.5 and 47.4 PVs, respectively. Dash lines represent the further division of Phase I and Phase II (Phases I-A, I-B, and I-C, and Phases II-A, II-B, and II-C), based on the observed differences in 6:2 FTS biotransformation behaviors. All columns were operated for a total of 305 days (136 days in Phase I and 169 days in Phase II). Error bars represent the standard error of duplicate abiotic and biotic columns.

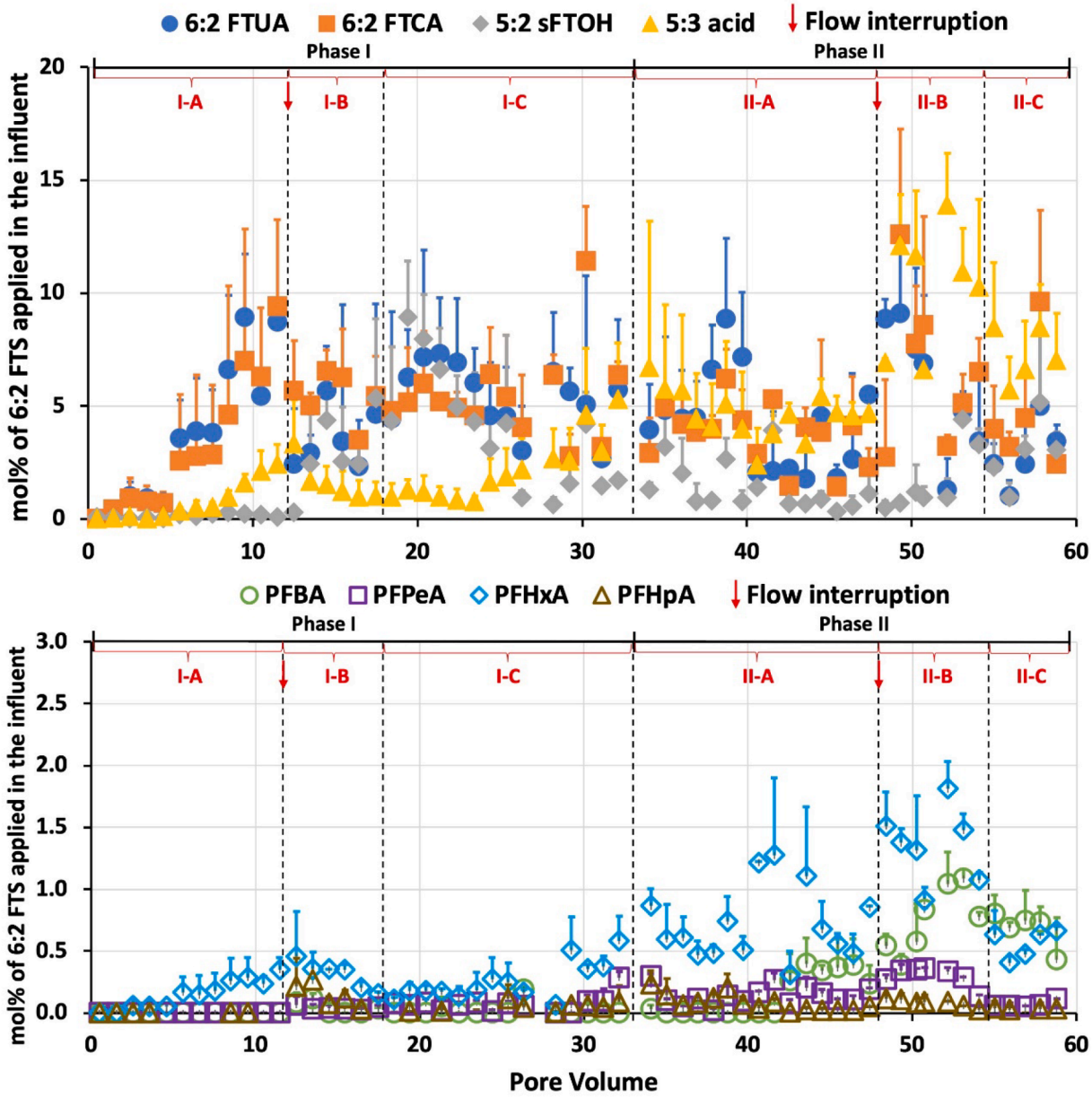


**Fig. 3.** Time-courses of 6:2 FTS biotransformation products in the effluent of biotic columns. A description of each phase is given in the Fig. 2 caption. Error bars represent the standard error of duplicate biotic columns. Note that different y-axis scales were used in top and bottom plots.

% for PFHxA, and 0.0 ± 0.1 mol% for PFHpA (Fig. 3).

Column operation entered Phase II-A at 33.1 PVs, when the flow rate was reduced ($v_p$ = 2.4 ± 0.1 cm/day). Overall, lower 6:2 FTS concentrations were observed in Phase II-A (33.1–47.4 PVs) than in Phase I-C (Fig. 2). On average, 55.4 ± 15.0 mol% and 70.8 ± 11.9 mol% of 6:2 FTS were measured in the effluent of the biotic columns during Phase II-A and Phase I-C, respectively. As for the biotransformation products, lower concentrations of early-stage products but increased concentrations of late-stage products were observed in Phase II-A compared to Phase I-C (Fig. 3). For example, the average molar yield of PFHxA during Phase II-A (0.7 ± 0.4 mol%) was more than tripled compared to Phase I-C (0.2 ± 0.2 mol%). These results indicate that the longer residence time during Phase II-A facilitated a more complete biotransformation of 6:2 FTS compared to Phase I-C.

At 47.4 PVs, a longer flow interruption of 7 days was performed. Immediately after resuming flow, side-ports samples were collected for ORP measurements (569.5 ± 22.7 mV; values reported relative to standard hydrogen electrode), which confirmed the maintenance of oxic conditions during the flow interruption (Table S3). In Phase II-B (47.4–54.1 PVs) following flow resumption, a substantial increase in the formation of 6:2 FTS biotransformation products was observed (Fig. 3), along with a decrease in average 6:2 FTS concentrations from 55.4 ± 15.0 mol% in Phase II-A to 45.1 ± 17.3 mol% in Phase II-B (Fig. 2). Average molar yields of 5:3 acid (10.4 ± 3.4 mol%), PFBA (0.7 ± 0.3 mol%), PFPeA (0.3 ± 0.1 mol%), and PFHxA (1.4 ± 0.4 mol%) in Phase II-B all more than doubled compared to Phase II-A (Fig. 3). Even the early-stage products, 6:2 FTCA and 6:2 FTUA were formed with higher molar yields (6.6 ± 4.0 and 6.0 ± 4.1mol%, respectively) in Phase II-B compared to Phase II-A (Fig. 3). Taken together, the biotransformation extent of 6:2 FTS was greatly enhanced by the 7-day flow interruption, resulting in a greater production of all 6:2 FTS transformation products in Phase II-B.

The extent of enhanced biotransformation following flow interruption appeared to be minimal after 54.1 PVs, as the production of biotransformation products in Phase II-C (54.1–58.8 PVs) returned to a similar level observed in Phase II-A (Fig. 3). The combined average

molar yield of early-stage products was 7.9 ± 5.2 mol% in Phase II-A, and 7.6 ± 6.0 mol% in Phase II-C. The combined average molar yield of late-stage products was 1.0 ± 0.8 mol% in Phase II-A, and 1.4 ± 0.3 mol% in Phase II-C. Moreover, similar concentrations of 6:2 FTS, 55.4 ± 15.0 and 52.3 ± 5.8 mol% were measured in Phase II-A and Phase II-C, respectively (Fig. 2). These findings suggest that Phase II-A and Phase II-C may represent steady-state 6:2 FTS biotransformation under the slower tested flow rate ($v_p$ = 2.4 ± 0.1 cm/day).

The average molar percent of 6:2 FTS and biotransformation products at each subphase discussed above are summarized in Table S4. A greater extent of 6:2 FTS biotransformation was achieved in Phase II compared to Phase I. By reducing the $v_p$ from 3.7 to 2.4 cm/day (35.1% reduction), the average molar percent of 6:2 FTS in Phases II-A and II-C were 21.7 % and 26.1 % lower than that in Phase I-C (Table S4). Correspondingly, fewer early-stage products but more late-stage products were produced in Phases II-A and II-C than Phase I-C (Table S4). Substantial enhancement of 6:2 FTS biotransformation extent was observed in Phases I-B and II-B following flow interruption, with the effects of both 2-day and 7-day flow interruptions persisting for 6–7 PVs after flow resumption (Figs. 2 and 3). Overall, these findings reveal that the 6:2 FTS biotransformation was rate-limited under the tested column conditions.

### 3.1.2. Biotransformation of 6:2 FTS along the flow path

A total of 14 sets of side-port samples were collected during different subphases (Table S1) to explore 6:2 FTS biotransformation along the flow path. To represent the extent of 6:2 FTS biotransformation occurring along the flow path, the molar percent of 6:2 FTS and biotransformation products in the side-port and effluent samples collected from the respective subphases were averaged, based upon the overall small variation (Fig. 4). The average molar percent of each compound was then compared among Ports 1–3 and effluent samples to depict the 6:2 FTS biotransformation extent along the flow path (Fig. 4).

In general, there was a decreasing trend in 6:2 FTS concentration along the flow path in each subphase (Fig. 4). During Phase I-C, 6:2 FTS decreased from 74.9 ± 10.9 mol% at Port 1 to 73.1 ± 12.8 mol% at Port 2, and further decreased to 61.3 ± 10.6 mol% at Port 3. Likewise, 6:2 FTS in Ports 1–3 and effluent samples during Phase II-C were 65.9 ± 6.3, 64.6 ± 1.7, 62.7 ± 7.3, and 55.6 ± 2.9 mol%, respectively (Fig. 4). Correspondingly, increasing trends in early and middle-stage products along the flow path were observed (Fig. 4). For example, during Phase I-C, 6:2 FTCA and 6:2 FTUA gradually increased from 1.5 ± 2.1 and 2.6 ± 0.9 mol% at Port 1, to 6.4 ± 2.7 and 5.6 ± 1.6 mol% in the effluent, respectively (Fig. 4). Similarly, 5:2 sFTOH and 5:3 acid gradually increased from 1.3 ± 0.5 and 1.8 ± 1.0 mol% at Port 1, to 1.8 ± 1.4 and 3.2 ± 2.3 mol% in the effluent, respectively (Fig. 4).

Although the biotransformation of 6:2 FTS was shown to increase along the flow path, an increasing trend in late-stage transformation products was not observed (Fig. 4). For example, during Phase II-A, average molar yields of PFHxA in Ports 1–3 and effluent samples were 1.1 ± 0.5, 0.8 ± 0.4, 1.2 ± 0.6, and 0.8 ± 0.4 mol%, respectively (Fig. 4). Meanwhile, the molar yields of each PFBA, PFPeA, and PFHpA remained in the range of 0.1–0.3 mol% across Ports 1–3 and effluent samples (Fig. 4). The stable late-stage products along the flow path could be attributed to the relatively short RTs in the columns. Despite the increase from 4.1 days in Phase I to 6.3 days in Phase II, the RT was likely much shorter than that needed for a substantial production of late-stage products (Yan et al., 2024).

Another unexpected finding was that 6:2 FTS biotransformation in the first quarter of the column (i.e., from column inlet to Port 1) represented a majority of the overall biotransformation extent (Fig. 4). In Phases I-C, II-A, II-B, and II-C, 6:2 FTS decreased by 25.1–43.2 % at Port 1 compared to the influent, while it only decreased an additional 5.9–26.7 % in the effluent compared to Port 1 (Fig. 4). In addition, molar yields of most of the quantified biotransformation products measured at Port 1 accounted for more than half of the total yields measured in the effluent (Fig. 4); although, the distance from Port 1 to the column outlet was 3-fold longer than that from the inlet to Port 1 (Fig. 1a). These results suggested that the first several 6:2 FTS biotransformation steps to form 6:2 FTCA, 6:2 FTUA, 5:2 sFTOH, and 5:3 acid occurred rapidly in the first quarter of the flow path. After this point, the biotransformation occurred relatively slowly, resulting in less 6:2 FTS decrease and biotransformation product formation downgradient of Port 1. The slower biotransformation of 6:2 FTS could be attributed to the formation of 6:2 FTCA and 6:2 FTUA in the first quarter of the column that may have resulted in microbial toxicity, as previously documented (Mitchell et al., 2011; Phillips et al., 2007). The non-uniform distribution of 6:2 FTS concentrations along the flow path, with the highest levels near the inlet, could have also contributed to the elevated transformation rate observed in the first quarter of columns.

### 3.1.3. Comparison of 6:2 FTS biotransformation between microcosm and column experiments

*3.1.3.1. Comparison of 6:2 FTS biotransformation rates.* To facilitate a comparison of 6:2 FTS biotransformation rate in the columns to the microcosms (Yan et al., 2024), mathematical modeling was undertaken to calculate rate coefficients for the initial step of 6:2 FTS biotransformation. Equation (1) was used to fit the evolution of 6:2 FTS concentration in the microcosms (SM-Section S3, Fig. S2), which yielded a reaction rate coefficient ($k$) of 0.137 ± 0.023 $cm^3_w/g_s/d$. The analytical solution to Equation (2) was applied to model the two steady-state phases, Phases I-C and II-A, in the column experiments (SM-Section S3). The $k$ of 0.039 ± 0.008 $cm^3_w/g_s/d$ was obtained for Phase I-C, which was not significantly different from $k$ of 0.041 ± 0.006 $cm^3_w/g_s/d$ for Phase II-A ($p$ = 0.65). The results indicated that the rate of 6:2 FTS biotransformation was independent of $v_p$ during the experiments. In other words, the greater biotransformation extent observed during Phase II-A compared to Phase I-C was attributed to the larger residence time (4.1 vs. 6.3 days).

The overall value of $k$ obtained for 6:2 FTS in the columns was ~3.5 times smaller than that fitted to microcosm data (0.039–0.041 vs 0.137 $cm^3_w/g_s/d$). However, if the model is modified to only consider 6:2 FTS biotransformation in the first quarter of the column (consistent with flow path measurements, Section 3.1.2), the fitted value of $k$ is 0.168 ± 0.020 $cm^3_w/g_s/d$, which is not significantly different ($p$ = 0.48) from the rate coefficient obtained in the microcosms ($k$ = 0.137 ± 0.023 $cm^3_w/g_s/d$).

Fig. 5 compares the measured 6:2 FTS concentrations in the column effluent and predictions from the transient transport model (Equation 2). Here, dispersion/diffusion ($D$) and sorption partition ($K_d$) coefficients were obtained by fitting the breakthrough curves from the tracer and 6:2 FTS abiotic column experiments, respectively. The reactive transport model used the $k$ obtained from steady-state analyses assuming that only the first quarter of the column was active for 6:2 FTS biotransformation. Although the model reflects the general trend of observations, it did not capture the initial acclimation period and the greater biotransformation extent observed after the first flow interruption. These results highlight the need to account for changes in the amount and distribution of biomass over time (Fitzgerald et al., 2019; Hnatko et al., 2023; Yang et al., 2021).

*3.1.3.2. Comparison of 6:2 FTS biotransformation extent and pathways.* In addition to the rate of the initial biotransformation step, the overall extent of 6:2 FTS biotransformation in the columns was compared to the microcosms (Yan et al., 2024), based on the residual 6:2 FTS and transformation products formation. As shown in Tables S4 and S5, residual 6:2 FTS and total mass recovery in Phase I-C fell within the range observed between day 7 and 28 microcosms. This suggests that the extent of 6:2 FTS biotransformation in steady-state Phase I-C (RT = 4.1 ± 0.2 days) was comparable to that occurred between day 7 and 28

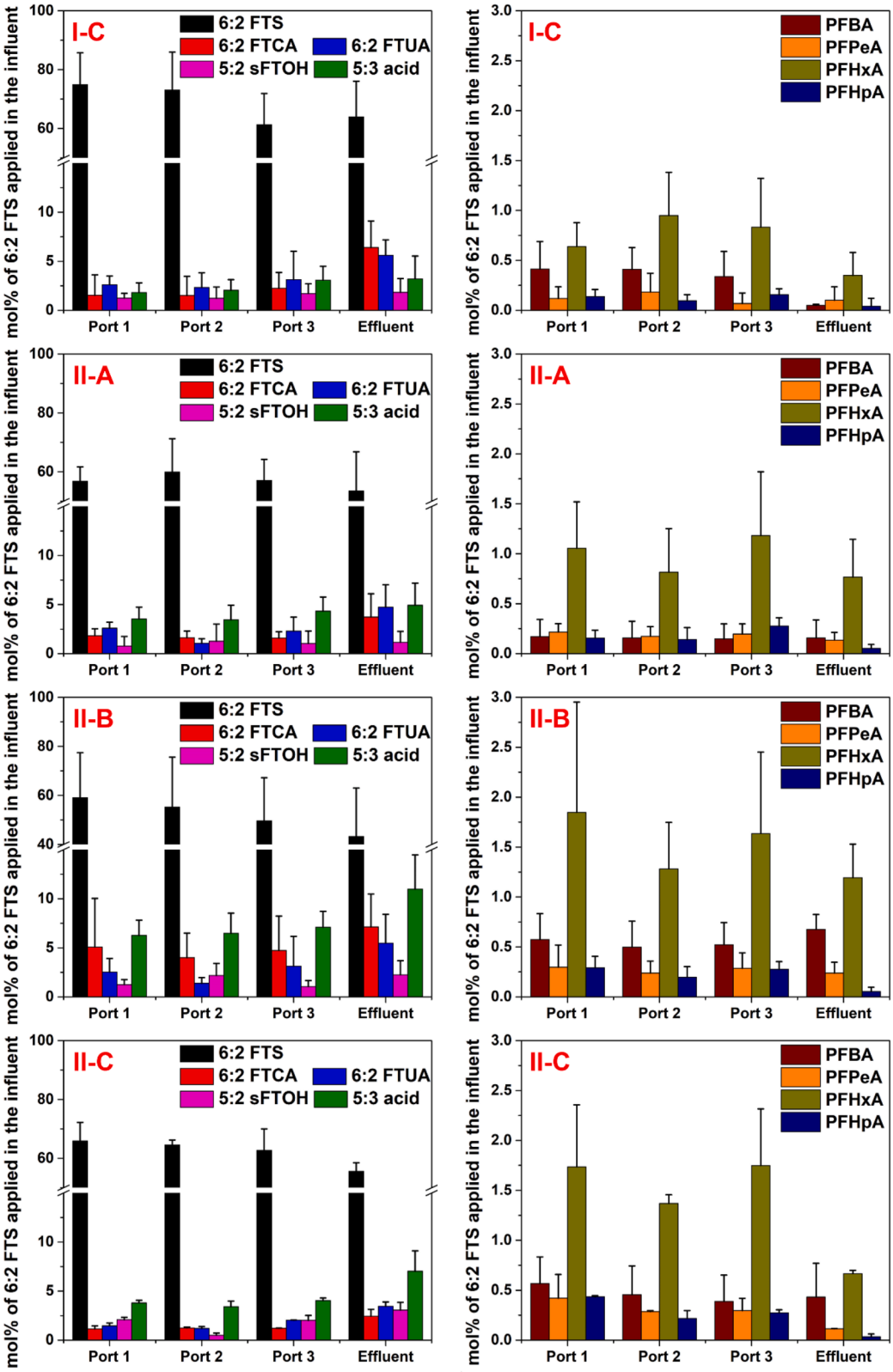


**Fig. 4.** The average molar percent of 6:2 FTS and biotransformation products along the flow path (i.e., Port 1, Port 2, Port 3, and Effluent, See Fig. 1) in different subphases. A description of each phase is given in the Fig. 2 caption. Phases I-A and I-B were not included because the initial side-port sampling technique did not acccurately capture PFAS samples within the flow path.

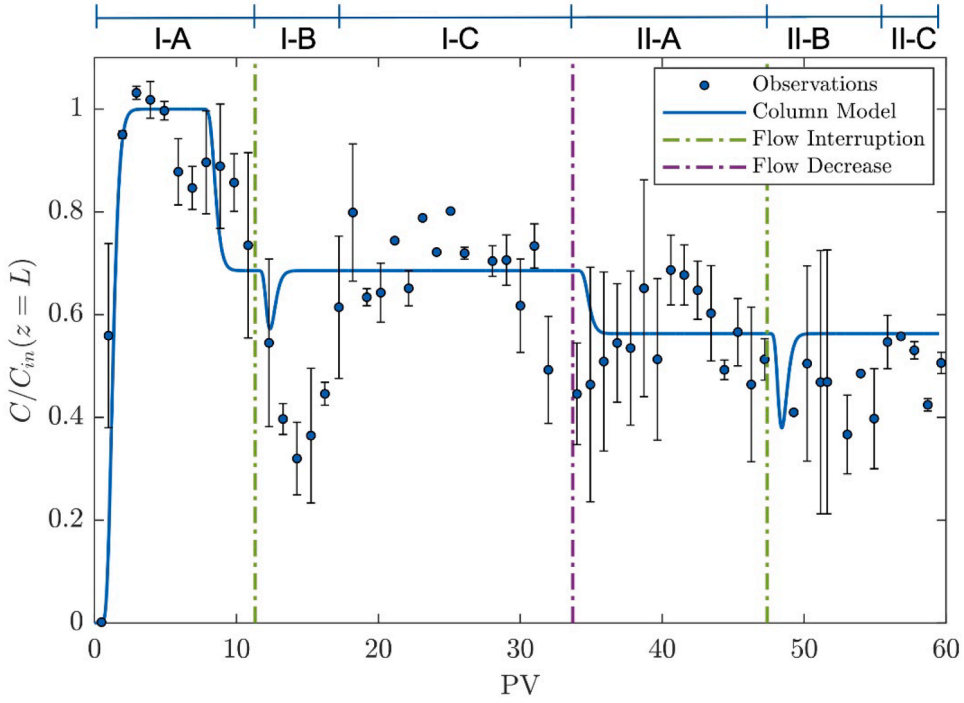


**Fig. 5.** Comparison of simulation and measured relative concentration of 6:2 FTS in the effluent, normalized by the influent concentration in column systems. Observations and model predictions use the reaction rate coefficient fitted from steady-state conditions assuming that only the first quarter of the column is active for 6:2 FTS biotransformation. The model also assumes an acclimation period of 7 PVs with no relevant microbial activity.

microcosms. Likewise, the extent of 6:2 FTS biotransformation in steady-state Phases II-A and II-C (RT = 6.3 ± 0.3 days) was similar to that occurred between day 28 and 56 microcosms (Tables S4 and S5). These findings indicated that the same extent of 6:2 FTS biotransformation was achieved more rapidly in the columns than in microcosms (4.1–6.3 days vs. 7–56 days). The extent of microbial dechlorination was also reported to be greater in continuous flow columns compared to batch reactors (Schaefer et al., 2009).

The biotransformation pathways of 6:2 FTS in the columns were found to be different from those in the microcosms. First, greater production of early-stage products was observed in the columns (Tables S4 and S5); combined molar yield of 6:2 FTCA and 6:2 FTUA in column experiments was 7.6–12.6 mol%, which was much higher than that in the microcosms (<3.7 mol%). Second, the biotransformation of 6:2 FTUA to 5:2 sFTOH was preferred over the conversion to 5:3 acid in the microcosms, with a greater molar yield of 5:2 sFTOH compared to 5:3 acid during the incubation, especially in first 56 days (Table S5). However, in the columns, the reverse preference of conversion to 5:3 acid over 5:2 sFTOH was found in Phase II (Fig. 3, Table S4). Finally, PFPeA and PFHxA were the two primary late-stage products in the microcosms (Table S5). However, PFPeA was not a main product in the columns (<0.3 ml%); instead, PFBA was more abundant (~0.7 mol% in Phases II-B and II-C) (Fig. 3, Table S4). Taken together, these findings suggested that system scale, solid-to-water ratio and/or flow conditions could impact the observed rate, extent, and/or pathways of 6:2 FTS biotransformation.

### *3.2. Dynamics of microbial communities throughout the column experiments*

#### *3.2.1. Diversity of microbial communities*

The microbial communities present in aqueous side-port samples collected during Phase I and Phase II, and solid samples from column segments S1-S5 collected upon the termination of experiments, are referred to hereafter as planktonic and porous media-attached microbial communities, respectively. Diversity and richness of these microbial communities were evaluated by the Shannon index and Chao1 index, respectively (Table S6). No significant differences ($p > 0.05$) in Shannon indices were found among Phases I or II side-port samples (Table S6), indicating the stable planktonic microbial diversity throughout the columns. Higher Chao1 indices were observed in Port 3 than Ports 1 and 2 (Table S6), suggesting greater planktonic microbial taxa closer to column outlet. Moreover, no significant differences ($p > 0.05$) in Shannon and Chao 1 indices were found among solid-phase samples from segments S1-S5 (Table S6), indicating consistent diversity and richness of attached microbial communities along the flow path. However, attached microbial communities exhibited significantly ($p < 0.05$) higher richness and diversity (Chao 1 and Shannon indices of 324.0 ± 48.9 and 4.6 ± 0.3, respectively) than planktonic microbial communities (Chao 1 and Shannon indices of 97.4 ± 30.6 and 2.4 ± 0.3, respectively) (Table S6). This finding suggests that most of the native microorganisms derived from Loring soil were attached to the porous media throughout the experiments. In addition, the micro-environments around soil particles may protect the attached microbes from the adverse ambient environment (e.g., high PFAS concentration in the bulk aqueous phase), which assisted in maintaining attached microbial community diversity. Previous studies have reported that such micro-environments could be protective for microbial dechlorination in the presence of high PFAS concentration (38.7 mg/L PFAAs) (Hnatko et al., 2023) and low pH conditions (Yang et al., 2017). Principal coordinate analysis (PCoA) revealed that the composition between planktonic and attached microbial communities were highly distinct, based on the separation between the clusters of aqueous side-port samples and solid samples from segments S1-S5 (Fig. 6).

#### *3.2.2. Dynamics of planktonic microbial communities*

In Phases I and II of the column experiments, planktonic microbial communities were predominately composed of phyla Proteobacteria (85.8 ± 3.5 %) and Firmicutes (7.3 ± 1.7 %) (Fig. 7a,b). Genus *Pseudomonas* (belonging to Proteobacteria), in which most species are aerobes, was the predominant genus across Ports 1–3 samples in both phases (Fig. 8a,b), confirming that oxic conditions were maintained

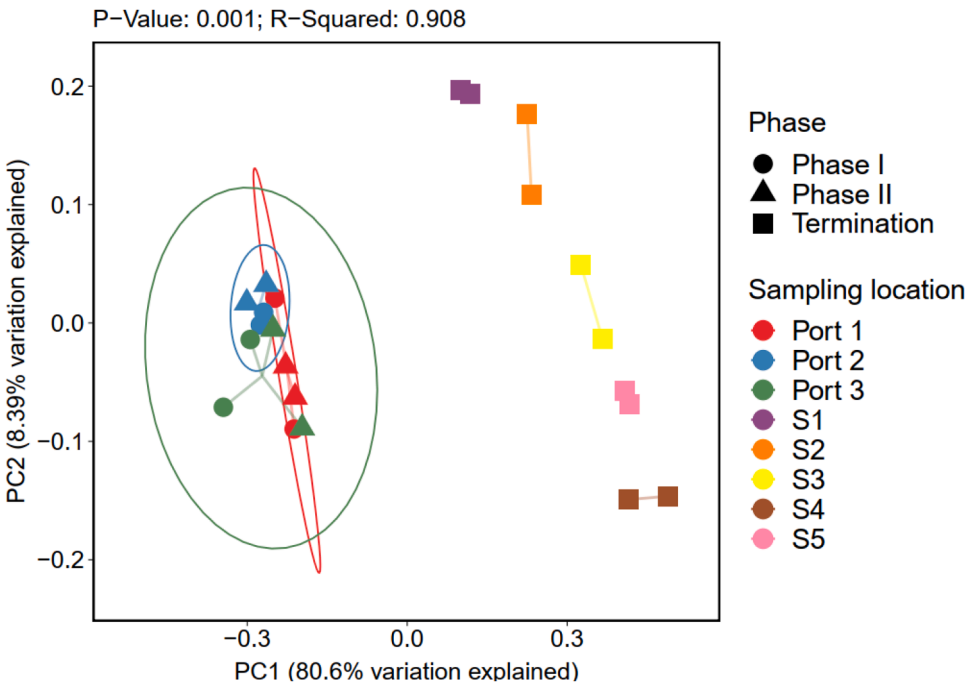


**Fig. 6.** Principal coordinate analysis (PCoA) plot based on microbial communities in aqueous side-port and solid samples from segments S1-S5. Each data point represents an individual sample. PCoA was calculated using weighted UniFrac distances. Samples collected at three side-ports and five segments along the column in Phase I, Phase II, and at the termination of the experiments are differentiated by color and shape. The ellipses represent 95 % confidence interval around the cluster centroid.

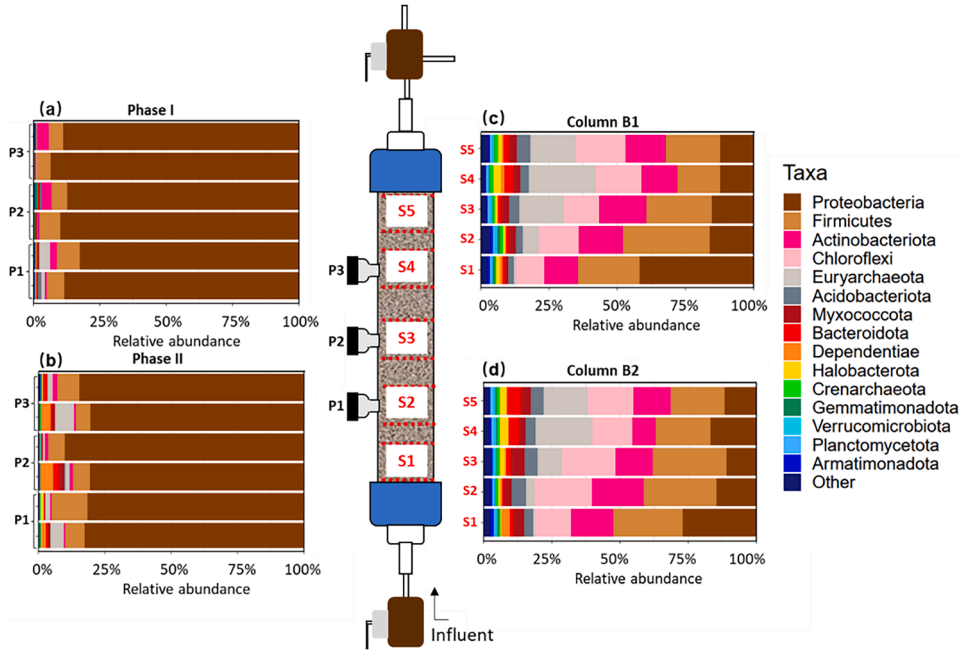


**Fig. 7.** Phylum-level composition of planktonic microbial communities in aqueous side-port samples collected during Phase I (a) and Phase II (b), and porous media-attached microbial communities in solid samples from segments S1-S5 of two biotic columns (c) (d).

throughout the experiments. Phyla Actinobacteriota (1.5 ± 0.5 %) and Desulfobacterota (7.3 ± 1.6 %) were also observed in planktonic microbial communities. Species in Proteobacteria, including *Pseudomonas, Brevundimonas, Afipia*, and *Herminiimonas,* known for biotransforming halogenated aromatic compounds, fluorinated alkanes or PFAS (Kim et al., 2014, 2012; Li et al., 2022; Xie et al., 2020; Yan et al., 2022) were found in Ports 1–3 samples with average relative abundances of 38.1 ± 7.6 %, 1.2 ± 1.0 %, 9.1 ± 5.4 %, and 4.5 ± 3.1 %, respectively. Additionally, Actinobacteriota and Desulfobacterota were reported to be potentially involved in 6:2 FTS biotransformation (Yan et al., 2024). These results indicate that planktonic microbial communities may play a role in the 6:2 FTS biotransformation.

The planktonic microbial community composition remained relatively stable among the Ports 1–3 or between two phases (Figs. 7 and 8) with minor shifts in certain taxa. For example, the average relative abundance of Actinobacteriota in Ports 1–2 was 1.7 ± 0.4 % but

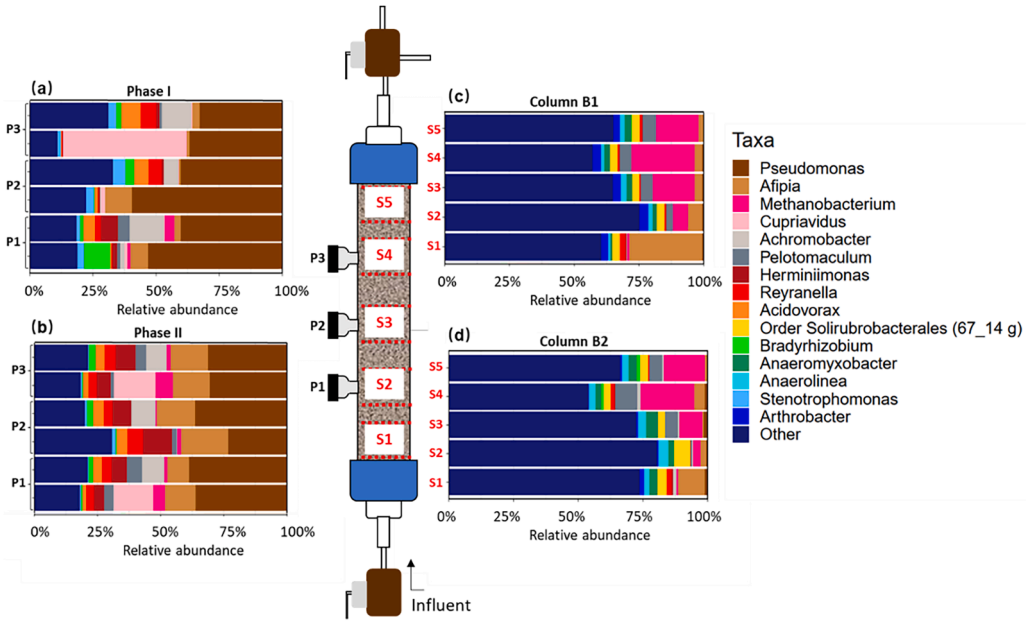


**Fig. 8.** Genus-level composition of planktonic microbial communities in aqueous side-port samples collected during Phase I (a) and Phase II (b), and porous media-attached microbial communities in solid samples from segments S1-S5 of two biotic columns (c) (d).

decreased to 1.1 ± 0.5 % in Port 3. Genus *Pseudomonas* had a higher average abundance in Phase I (43.7 ± 6.5 %) than Phase II (32.6 ± 3.4 %). These shifts might be related to the associated sensitivity/tolerance to 6:2 FTS and biotransformation products. Compared to Phase I, planktonic microbial communities were exposed to a lower level of 6:2 FTS but higher levels of transformation products in Phase II. Some of the transformation products (e.g., 6:2 FTCA and 6:2 FTUA) are potentially more toxic to certain taxa in planktonic microbial community, as has been previously documented for higher-level organisms (Mitchell et al., 2011; Phillips et al., 2007).

### 3.2.3. *Spatial distribution of porous media-attached microbial communities*

At the conclusion of the 305-day column experiments, the dominant microbial taxa in column segments S1-S5 included four bacterial phyla, Firmicutes (23.3 ± 4.1 %), Proteobacteria (17.8 ± 8.3 %), Chloroflexi (15.8 ± 2.2 %), Actinobacteriota (14.4 ± 2.2 %), and one archaeal phylum Euryarchaeota (11.4 ± 7.9 %). These five phyla accounted for a significant proportion (79.8–84.8 %) of the attached microbial communities (Fig. 7c,d). Some species in phyla Proteobacteria and Actinobacteriota are known fluorotelomer degraders (Kim et al., 2014, 2012; Van Hamme et al., 2013; Yang et al., 2022). Firmicutes and Chloroflexi were found capable of biotransforming chlorinated solvents and other organohalides (Krzmarzick et al., 2014, 2012). In addition, all five phyla were previously reported to be abundant in PFAS-contaminated soils (Li et al., 2017). Therefore, the dominance of these phyla throughout the columns suggested their higher tolerance to 6:2 FTS and biotransformation products, as well as their potential ability to transform 6:2 FTS.

Differences in microbial community composition among segments S1-S5 were further investigated to provide insights into how attached microbial communities shifted along the flow path. As illustrated in Fig. 7, the relative abundances of Firmicutes and Proteobacteria decreased from the column inlet (23.9 ± 1.3 % and 34.4 ± 7.3 % in S1, respectively) to the outlet (19.9 ± 0.1 % and 11.9 ± 0.2 % in S5, respectively). Conversely, phyla such as Euryarchaeota (0.9 ± 0.2 % and 16.3 ± 0.2 % in S1 and S5, respectively) and Halobacterota (1.0 ± 0.4 % and 2.0 ± 0.5 % in S1 and S5, respectively) were more abundant at the locations close to the outlet than the inlet (Fig. 7c,d). Examining attached microbial communities more closely on the genus level revealed that the relative abundance of genus *Methanobacterium* increased significantly ($p < 0.05$) from the inlet (0.9 ± 0.2 % in S1) to the outlet (16.3 ± 0.2 % in S5) (Fig. 8c,d). Also, genus *Pelotomaculum* was significantly ($p < 0.05$) more abundant in the segment closest to the outlet (5.0 ± 0.1 % in S5) compared to the segment closest to the inlet (<0.1 % in S1). Increasing trends in relative abundance from segments S1 to S5 were also observed for genera *Levilinea* (0.3 ± 0.1 % in S1, and 1.0 ± 0.0 % in S5) and *Methanospirillum* (0 % in S1, and 0.3 ± 0.2 % in S5). In contrast, decreasing trends from segments S1 to S5 were observed for genera such as *Rhodococcus* (0.7 ± 0.2 % in S1, and <0.1 % in S5) and *Actinotalea* (0.4 ± 0.0 % in S1, and 0 % in S5).

The shifts in attached microbial communities along the flow path could be attributed to several factors. First, while maintaining oxic conditions, the potential gradual decrease in oxygen levels from segments S1 to S5 might lead to the increase in facultative and anaerobic microorganisms (e.g., *Methanobacterium* and *Methanospirillum*, as discussed above) towards the outlet end of the column. Second, 6:2 FTS biotransformation along the flow path exposed attached microbial communities in segments S1-S5 to different concentrations of various PFAS for an extended period (i.e., 305 days). For example, the microbial communities in segment S1 were exposed to higher concentrations of 6:2 FTS than those in segment S5, while segment S5 was exposed to higher levels of 6:2 FTS biotransformation products than segment S1. Therefore, the extent of tolerance to those various PFAS by attached microbial communities species played a role in shaping their spatial distribution. Genus *Levilinea* was previously reported to increase in river sediment after exposure to 6:2 fluorotelomer alcohol (Zhang et al., 2017), an intermediate of 6:2 FTS biotransformation. The tolerance of *Levilinea* to 6:2 FTS biotransformation products could explain its increase in relative abundance from segments S1 to S5. Lastly, shifts in some genera along the flow path could be due to their involvement in specific 6:2 FTS biotransformation stages. The decrease in genus *Rhodococcus* from segments S1 to S5 may be linked to its role in the early-stage of 6:2 FTS biotransformation (Yang et al., 2022), while the increase in genus *Pelotomaculum* along the flow path suggests its potential involvement in the later stage of 6:2 FTS biotransformation (Dong et al., 2017).

## 4. Conclusion

This study investigated the biotransformation of 6:2 FTS and associated dynamics of microbial communities in 305-day flow-through column experiments packed with saturated soil from an AFFF-impacted site. A reduction in $v_p$ from 3.7 to 2.4 cm/day resulted in a 21.7–26.1 % decrease in effluent concentrations of 6:2 FTS, lower yields of 6:2 FTCA and 6:2 FTUA, and greater yields of $C_4$–$C_7$ PFCAs. In addition, 2 and 7-day flow interruptions enhanced the biotransformation of 6:2 FTS after the resumption of flow. Throughout the 305-day experiments, distinct differences between planktonic and attached microbial communities in the columns were observed. Microbial taxa that potentially played a role in 6:2 FTS biotransformation included *Pseudomonas* in planktonic microbial communities, and *Rhodococcus* and *Pelotomaculum* in attached microbial communities.

In comparison with prior microcosms, greater 6:2 FTS biotransformation extent and different biotransformation pathways were observed in the present dynamic columns. Mathematic modelling estimated 6:2 FTS biotransformation rates in the column experiments to be 0.039–0.041 $cm^3_w/g_s/d$, which were around 3.5-time smaller than microcosm-fitted coefficients ($0.137 \pm 0.023$ $cm^3_w/g_s/d$). These findings emphasize the importance of accounting for experimental system scale and conditions (resembling that of the field with water flow and porous medium) when assessing the fate and transformation of 6:2 FTS in the natural environment. Given that almost all studies to-date on PFAS biotransformation have been conducted in batch reactor experiments, future research to investigate PFAS biotransformation in more realistic systems that incorporate important environmental conditions (e.g., water flow, saturated and unsaturated zones) are urgently needed.

## CRediT authorship contribution statement

**Peng-Fei Yan:** Investigation, Methodology, Visualization, Writing – original draft, Writing – review & editing. **Sheng Dong:** Investigation, Methodology, Visualization, Writing – review & editing, Writing – original draft. **Matthew J. Woodcock:** Resources, Writing – review & editing. **Katherine E. Manz:** Resources, Writing – review & editing. **Uriel Garza-Rubalcava:** Resources, Writing – review & editing. **Linda M. Abriola:** Funding acquisition, Writing – review & editing. **Kurt D. Pennell:** Funding acquisition, Writing – review & editing. **Natalie L. Cápiro:** Conceptualization, Funding acquisition, Supervision, Writing – review & editing.

## Declaration of competing interest

The authors declare that they have no known competing financial interests or personal relationships that could have appeared to influence the work reported in this paper.

## Data availability

Data will be made available on request.

## Acknowledgements

This study was supported by the Strategic Environmental Research and Development Program (SERDP) under contract W912HQ-18-C-0014 for Project ER18–1149, "Development and Laboratory Validation of Mathematical Modeling Tools for Prediction of PFAS Transformation, Transport, and Retention in AFFF Source Areas". We acknowledge Naji Akladiss at Maine Department of Environmental Protection for providing access to collect Loring soil. Peng-Fei Yan and Sheng Dong also acknowledge the financial support from the China Scholarship Council, and Auburn University Graduate School and Office of International Programs.

## Supplementary materials

Supplementary material associated with this article can be found, in the online version, at doi:10.1016/j.watres.2024.121146.

## References

Ahrens, L., Norström, K., Viktor, T., Cousins, A.P., Josefsson, S., 2015. Stockholm Arlanda Airport as a source of per- and polyfluoroalkyl substances to water, sediment and fish. Chemosphere, Per- and Polyfluorinated Alkyl substances (PFASs) in materials, humans and the environment – current knowledge and scientific gaps. 129, 33–38. https://doi.org/10.1016/j.chemosphere.2014.03.136.

Buck, R.C., Franklin, J., Berger, U., Conder, J.M., Cousins, I.T., de Voogt, P., Jensen, A.A., Kannan, K., Mabury, S.A., van Leeuwen, S.P., 2011. Perfluoroalkyl and polyfluoroalkyl substances in the environment: terminology, classification, and origins. Integr. Environ. Assess. Manag. 7, 513–541. https://doi.org/10.1002/ieam.258.

Dong, S., Yan, P.-F., Liu, C., Manz, K.E., Mezzari, M.P., Abriola, L.M., Pennell, K.D., Cápiro, N.L., 2023. Assessing aerobic biotransformation of 8:2 fluorotelomer alcohol in aqueous film-forming foam (AFFF)-impacted soils: pathways and microbial community dynamics. J. Hazard. Mater. 446, 130629 https://doi.org/10.1016/j.jhazmat.2022.130629.

Dong, X., Dröge, J., von Toerne, C., Marozava, S., McHardy, A.C., Meckenstock, R.U., 2017. Reconstructing metabolic pathways of a member of the genus Pelotomaculum suggesting its potential to oxidize benzene to carbon dioxide with direct reduction of sulfate. FEMS Microbiol. Ecol. 93, fiw254. https://doi.org/10.1093/femsec/fiw254.

Fitzgerald, N.J.M., Temme, H.R., Simcik, M.F., Novak, P.J., 2019. Aqueous film forming foam and associated perfluoroalkyl substances inhibit methane production and Co-contaminant degradation in an anaerobic microbial community. Environ. Sci.: Processes Impacts 21, 1915–1925. https://doi.org/10.1039/C9EM00241C.

Grandjean, P., Clapp, R., 2015. Perfluorinated Alkyl substances: emerging insights into health risks. New Solut 25, 147–163. https://doi.org/10.1177/1048291115590506.

Grösbacher, M., Eckert, D., Cirpka, O.A., Griebler, C., 2018. Contaminant concentration versus flow velocity: drivers of biodegradation and microbial growth in groundwater model systems. Biodegradation 29, 211–232. https://doi.org/10.1007/s10532-018-9824-2.

Hamid, H., Li, L.Y., Grace, J.R., 2020. Aerobic biotransformation of fluorotelomer compounds in landfill leachate-sediment. Sci. Total Environ. 713, 136547 https://doi.org/10.1016/j.scitotenv.2020.136547.

Han, K., Levenspiel, O., 1988. Extended monod kinetics for substrate, product, and cell inhibition. Biotechnol. Bioeng. 32, 430–447. https://doi.org/10.1002/bit.260320404.

Hnatko, J.P., Liu, C., Elsey, J.L., Dong, S., Fortner, J.D., Pennell, K.D., Abriola, L.M., Cápiro, N.L., 2023. Microbial reductive dechlorination by a commercially available dechlorinating consortium is not inhibited by Perfluoroalkyl Acids (PFAAs) at field-relevant concentrations. Environ. Sci. Technol. https://doi.org/10.1021/acs.est.2c04815.

Houtz, E.F., Higgins, C.P., Field, J.A., Sedlak, D.L., 2013. Persistence of Perfluoroalkyl acid precursors in AFFF-impacted groundwater and soil. Environ. Sci. Technol. 47, 8187–8195. https://doi.org/10.1021/es4018877.

Kim, M.H., Wang, N., Chu, K.H., 2014. 6:2 Fluorotelomer alcohol (6:2 FTOH) biodegradation by multiple microbial species under different physiological conditions. Appl. Microbiol. Biotechnol. 98, 1831–1840. https://doi.org/10.1007/s00253-013-5131-3.

Kim, M.H., Wang, N., McDonald, T., Chu, K.-H., 2012. Biodefluorination and biotransformation of fluorotelomer alcohols by two alkane-degrading *Pseudomonas* strains. Biotechnol. Bioeng 109, 3041–3048. https://doi.org/10.1002/bit.24561.

Krzmarzick, M.J., Crary, B.B., Harding, J.J., Oyerinde, O.O., Leri, A.C., Myneni, S.C.B., Novak, P.J., 2012. Natural Niche for Organohalide-Respiring Chloroflexi. Appl. Environ. Microbiol. 78, 393–401. https://doi.org/10.1128/AEM.06510-11.

Krzmarzick, M.J., Miller, H.R., Yan, T., Novak, P.J., 2014. Novel firmicutes group implicated in the dechlorination of two chlorinated Xanthones, analogues of natural organochlorines. Appl. Environ. Microbiol. 80, 1210–1218. https://doi.org/10.1128/AEM.03472-13.

Li, B., Bao, Y., Xu, Y., Xie, S., Huang, J., 2017. Vertical distribution of microbial communities in soils contaminated by chromium and perfluoroalkyl substances. Sci. Environ. 599–600, 156–164. https://doi.org/10.1016/j.scitotenv.2017.04.241.

Li, Y.-J., Chuang, C.-H., Cheng, W.-C., Chen, S.-H., Chen, W.-L., Lin, Y.-J., Lin, C.-Y., Shih, Y., 2022. A metagenomics study of hexabromocyclododecane degradation with a soil microbial community. J. Hazard. Mater. 430, 128465 https://doi.org/10.1016/j.jhazmat.2022.128465.

Liu, M., Munoz, G., Vo Duy, S., Sauvé, S., Liu, J., 2021. Stability of Nitrogen-Containing Polyfluoroalkyl Substances in Aerobic Soils. Environ. Sci. Technol. acs.est.0c05811. https://doi.org/10.1021/acs.est.0c05811.

Mitchell, R.J., Myers, A.L., Mabury, S.A., Solomon, K.R., Sibley, P.K., 2011. Toxicity of fluorotelomer carboxylic acids to the algae Pseudokirchneriella subcapitata and Chlorella vulgaris, and the amphipod Hyalella azteca. Ecotoxicol. Environ. Saf. 74, 2260–2267. https://doi.org/10.1016/j.ecoenv.2011.07.034.

Moody, C.A., Field, J.A., 2000. Perfluorinated surfactants and the environmental implications of their use in fire-fighting foams. Environ. Sci. Technol. 34, 3864–3870. https://doi.org/10.1021/es991359u.

Nelson, J.W., Hatch, E.E., Webster, T.F., 2010. Exposure to Polyfluoroalkyl chemicals and cholesterol, body weight, and insulin resistance in the general U.S. population. Environ. Health Perspect. 118, 197–202. https://doi.org/10.1289/ehp.0901165.

Phillips, M.M.(MacDonald), Dinglasan-Panlilio, M.J.A., Mabury, S.A., Solomon, K.R., Sibley, P.K., 2007. Fluorotelomer acids are more toxic than Perfluorinated acids. Environ. Sci. Technol. 41, 7159–7163. https://doi.org/10.1021/es070734c.

Prevedouros, K., Cousins, I.T., Buck, R.C., Korzeniowski, S.H., 2006. Sources, fate and transport of Perfluorocarboxylates. Environ. Sci. Technol. 40, 32–44. https://doi.org/10.1021/es0512475.

Schaefer, C.E., Condee, C.W., Vainberg, S., Steffan, R.J., 2009. Bioaugmentation for chlorinated ethenes using Dehalococcoides sp.: comparison between batch and column experiments. Chemosphere 75, 141–148. https://doi.org/10.1016/j.chemosphere.2008.12.041.

Van Hamme, J.D., Bottos, E.M., Bilbey, N.J., Brewer, S.E., 2013. Genomic and proteomic characterization of Gordonia sp. NB4-1Y in relation to 6 : 2 fluorotelomer sulfonate biodegradation. Microbiology (N Y) 159, 1618–1628. https://doi.org/10.1099/mic.0.068932-0.

Xie, Y., Chen, G., May, A.L., Yan, J., Brown, L.P., Powers, J.B., Campagna, S.R., Löffler, F. E., 2020. Pseudomonas sp. strain 273 degrades fluorinated Alkanes. Environ. Sci. Technol. 54, 14994–15003. https://doi.org/10.1021/acs.est.0c04029.

Yan, P.-F., Dong, S., Manz, K.E., Liu, C., Woodcock, M.J., Mezzari, M.P., Abriola, L.M., Pennell, K.D., Cápiro, N.L., 2022. Biotransformation of 8:2 Fluorotelomer Alcohol in Soil from Aqueous Film-Forming Foams (AFFFs)-Impacted Sites under Nitrate-, Sulfate-, and Iron-reducing conditions. Environ. Sci. Technol. 56, 13728–13739. https://doi.org/10.1021/acs.est.2c03669.

Yan, P.-F., Dong, S., Manz, K.E., Woodcock, M.J., Liu, C., Mezzari, M.P., Abriola, L.M., Pennell, K.D., Cápiro, N.L., 2024. Aerobic biotransformation of 6:2 fluorotelomer sulfonate in soils from two aqueous film-forming foam (AFFF)-impacted sites. Water Res. 249, 120941 https://doi.org/10.1016/j.watres.2023.120941.

Yang, L., Hnatko, J.P., Elsey, J.L., Christ, J.A., Pennell, K.D., Cápiro, N.L., Abriola, L.M., 2021. Exploration of processes governing microbial reductive dechlorination in a heterogeneous aquifer flow cell. Water Res. 193, 116842 https://doi.org/10.1016/j.watres.2021.116842.

Yang, S.-H., Shi, Y., Strynar, M., Chu, K.-H., 2022. Desulfonation and defluorination of 6:2 fluorotelomer sulfonic acid (6:2 FTSA) by Rhodococcus jostii RHA1: carbon and sulfur sources, enzymes, and pathways. J. Hazard. Mater. 423, 127052 https://doi.org/10.1016/j.jhazmat.2021.127052.

Yang, Y., Cápiro, N.L., Marcet, T.F., Yan, J., Pennell, K.D., Löffler, F.E., 2017. Organohalide respiration with chlorinated Ethenes under low pH conditions. Environ. Sci. Technol. 51, 8579–8588. https://doi.org/10.1021/acs.est.7b01510.

Zhang, S., Lu, X., Wang, N., Buck, R.C., 2016. Biotransformation potential of 6:2 fluorotelomer sulfonate (6:2 FTSA) in aerobic and anaerobic sediment. Chemosphere 154, 224–230. https://doi.org/10.1016/j.chemosphere.2016.03.062.

Zhang, S., Merino, N., Wang, N., Ruan, T., Lu, X., 2017. Impact of 6:2 fluorotelomer alcohol aerobic biotransformation on a sediment microbial community. Sci. Total Environ. 575, 1361–1368. https://doi.org/10.1016/j.scitotenv.2016.09.214.